

Annealing of Electron Bombardment Damage in Silicon Crystals

G. BEMSKI AND W. M. AUGUSTYNIAK
Bell Telephone Laboratories, Murray Hill, New Jersey
 (Received July 17, 1957)

Silicon crystals were bombarded at room temperature with electrons of 700 kev from a Van de Graaff accelerator. The annealing of the bombardment damage was studied between 200°C and 400°C by observing the recovery of the minority-carrier lifetime. The annealing was found to proceed with an activation energy of 1.3 ev. This is interpreted as being the activation energy associated with the lattice jump frequency.

The kinetics of the annealing are identical in most *p*-type and *n*-type crystals. A second-order process has been identified toward the end of the annealing. Evidence is given that crystalline defects can influence the annealing kinetics.

I. INTRODUCTION

SEVERAL workers have studied the damage caused by electron bombardment in metals and semiconductors.^{1,2} The interest in such experiments became pronounced when it was realized³ that permanent changes in the crystal structure could be induced with an electron beam.

It is possible to divide the effects of electron bombardment into two general categories:

1. Excitation of electrons which, in semiconductors, results in an increase in the densities of free electrons and holes above their equilibrium values. The holes and electrons recombine with their characteristic lifetime which is, generally, less than 10^{-3} sec. This transient effect consumes a large part of the energy transferred by the bombarding electrons.
2. Displacement of stationary nuclei from their normal lattice positions which give rise to interstitials and vacancies. The present experiments deal with the second type of effect.

Several writers have shown⁴ that, in many cases, a displacement of atoms from their normal positions leads to a complex kind of damage, such as the formation of clusters, and localized heating of the lattice, leaving the crystal in a state in which the distribution of the induced defects is very nonuniform. This, however, happens mainly during bombardment with heavy particles which transfer a large momentum. Electrons, on the other hand, transfer a small momentum to the displaced atoms. The probability that such a displaced atom can produce further displacements is low. One should expect, therefore, that in its simplest form, the damage will consist of individual vacancy-interstitial pairs called Frenkel defects. There is evidence that such Frenkel defects are electrically active and introduce donor and acceptor energy levels within the energy gap

in germanium as well as in silicon.⁵ For that reason, resistivity measurements are frequently used to study the damage in semiconductors. The lifetime of minority carriers in silicon also can be used to study bombardment damage. Loferski and Rappaport⁶ have measured lifetime to determine the threshold for introduction of damage in germanium and silicon. Wertheim has found a recombination level in *n*-type silicon at 0.31 ev above the valence band.⁷ He further found that values of the capture cross section for holes and electrons in *n*-type silicon are 2.8×10^{-14} cm² and 10^{-16} cm², respectively.

In samples in which clustering can be neglected, the change in the rate of recombination, that is, the inverse of the lifetime, is proportional to the number of recombination centers introduced, so long as no pronounced changes in the Fermi level take place.⁸ Because of the fairly high capture cross section in bombarded silicon, it is possible to detect changes in the density of defects of the order of 10^{13} cm⁻³. Such small changes are very difficult to observe by resistivity measurements. The measurement of the lifetime of minority carriers is, therefore, well suited to the study of bombardment damage on "lightly" bombarded silicon in which the Fermi level does not change appreciably.

In the present experiments, measurements of lifetime have been used to study the annealing of bombardment damage. In these studies, the absolute density of defects introduced by bombardment is not of essential importance since the interpretation involves relative changes during the annealing cycle and most conclusions would be valid even without knowledge of the capture cross section. One needs only assume that the cross sections remain constant over the whole annealing cycle. From these studies one can acquire some knowledge concerning the character and the motion of the defects.

¹ G. J. Dienes, *Annual Review of Nuclear Sciences* (Annual Reviews, Inc., Stanford, 1953), Vol. 2, p. 187.

² F. Seitz and J. S. Koehler, in *Solid State Physics*, edited by F. Seitz and D. Turnbull (Academic Press, Inc., New York, 1956), Vol. 2, p. 307.

³ F. Seitz, *Phys. Today* 5, No. 6, 6 (1952).

⁴ J. A. Brinkman, *Am. J. Phys.* 24, 246 (1956).

⁵ H. Y. Fan and K. Lark-Horovitz, *Irradiation of Semiconductors*, Conference at Garmisch Partenkirchen, Germany, 1956 (unpublished).

⁶ J. J. Loferski and P. Rappaport, *Phys. Rev.* 98, 1861 (1955).

⁷ G. Wertheim, *Phys. Rev.* 105, 1730 (1957).

⁸ Hall-Shockley-Read model: W. Shockley and W. T. Read, *Phys. Rev.* 87, 835 (1952).

TABLE I. Summary of bombardment and annealing results.^a

| Crystal No. | ρ ohm cm | τ_0 μ sec | N_0 (total) flux electrons cm^{-2} | τ_b μ sec | η_s min | c_s | Comments |
|-------------|------------------|-----------------------|--|-----------------------|-----------------|-------|--|
| 1 | 8.5 <i>n</i> | 29 | 7.5×10^{15} | 0.3 | 200 | 0.15 | Pulled in He; rotation 0 rpm |
| 2 | 2.7 <i>p</i> | 12 | 3.3×10^{15} | 0.2 | 300 | 0.15 | Pulled in He; rotation 60 rpm |
| 3 | 13 <i>p</i> | 23 | 2.5×10^{15} | 2.0 | 1000 | 0.10 | Pulled in He; rotation 3 rpm |
| 4 | 10 <i>p</i> | 20 | 1.2×10^{14} | 1.8 | 2500 | 0.15 | Pulled in He; rotation 0 rpm |
| 5 | 3 <i>n</i> | 15 | 6.6×10^{14} | 3.0 | 1500 | 0.10 | Pulled in He; rotation 60 rpm |
| 6 | 9 <i>p</i> | 15 | 1.5×10^{15} | 0.6 | 600 | 0.15 | Pulled in He; rotation 0 rpm |
| 7 | 13 <i>p</i> | 15 | 4×10^{15} | 2.0 | 200 | 0.10 | Pulled in He; rotation 0 rpm |
| 8 | 80 <i>p</i> | 40 | 5×10^{15} | 0.8 | ... | 0.0 | Floating zone; grown in H_2 |
| 9 | 45 <i>p</i> | 45 | 8×10^{15} | 0.8 | 200 | 0.10 | Floating zone; grown in vacuum |
| 10 | 5.6 <i>n</i> | 15 | 2×10^{15} | 0.4 | 1000 | 0.35 | Pulled in He; rotation 60 rpm; 10^{15} copper atoms cm^{-3} |

^a The values of η_s listed are for an annealing temperature of 350°C.

II. EXPERIMENTAL PROCEDURE

a. Bombardment

Bombardments were made with a 700-keV electron beam from a Van de Graaff accelerator. Silicon samples were bombarded in groups of ten. By passing the electron beam through a 0.003-in. aluminum window approximately 3 in. in front of the samples, uniform exposure of the samples was achieved. The samples were turned over after being exposed to half of the total flux in order to expose both large-area surfaces to the beam and thus assure a uniform distribution of defects throughout the volume of the samples.

In a test experiment, it was established that up to a sample thickness of 0.020 in., the damage within a sample was uniform to $\pm 10\%$. The samples used here consisted of grown *p-n* junctions 0.017 in. thick. The bombardment took place in a vacuum of about 10^{-5} mm Hg. During the bombardment, the sample temperature remained below 75°C.

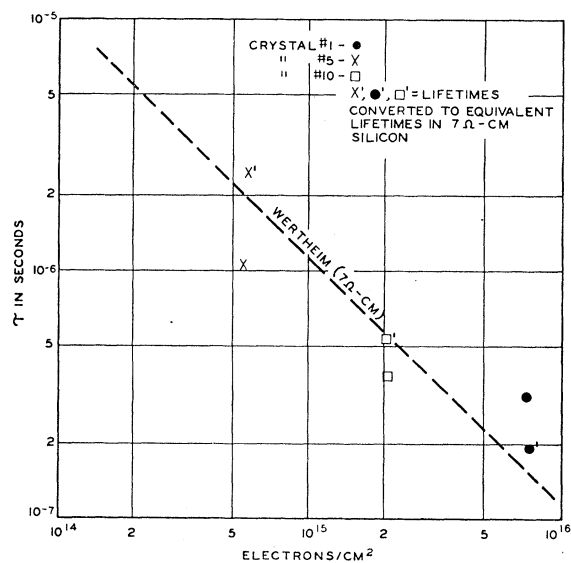


FIG. 1. Lifetime of holes in *n*-type silicon after bombardment as a function of total electron flux. Included is a comparison with Wertheim's results.

b. Annealing

The annealing was performed in an oil bath (Aroclor 1254, Monsanto Chemical Company) with a high-speed stirrer (3500 rpm) providing circulation of the bath. The temperature was controlled to $\pm 1^\circ\text{C}$. Two samples from one crystal were carried through a complete annealing cycle at a constant temperature.

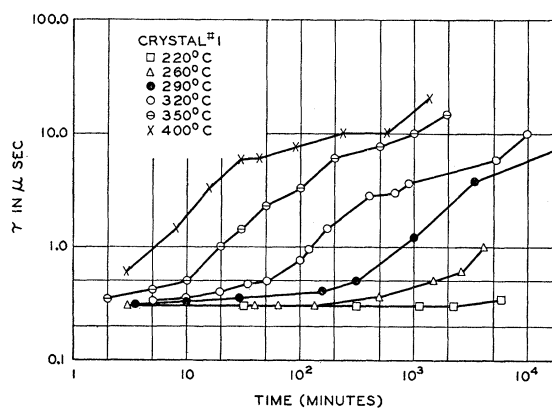


FIG. 2. Lifetimes obtained by annealing crystal No. 1 at different temperatures, as a function of time.

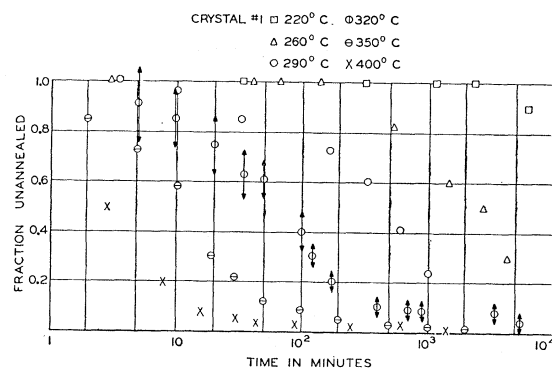


FIG. 3. Results of Fig. 2 expressed as a fraction of unannealed defects. The typical magnitude of errors is indicated for one set of points.

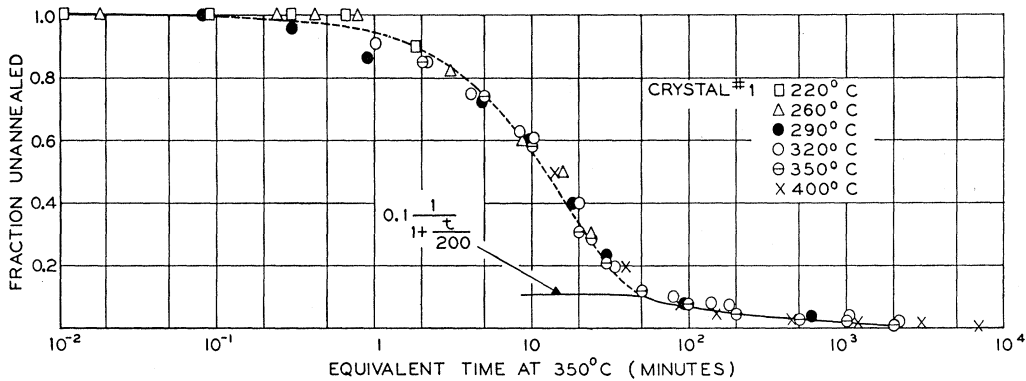


FIG. 4. Superposition of points in Fig. 3 by shifting the time scale. The data for 350°C were selected as a reference. The tail of the annealing curve is fitted with the second-order process.

c. Lifetime Measurements

The lifetime measurements were performed by the injection-extraction method.⁹ All the measurements were performed at room temperature. Necessary corrections for surface recombination velocity were applied in converting the observed lifetime to body lifetime. This correction became important only for lifetimes above 4 to 5 microseconds which were observed toward the end of the annealing. The error in lifetime measurements was estimated at $\pm 0.1 \mu\text{sec}$. The average of the values obtained on equivalent samples was used for the evaluations.

III. RESULTS

a. Bombardment

All the results are exhibited in Table I, where the starting resistivity, ρ , and lifetime, τ_0 , as well as mean life, τ_b , measured after the bombardment, are listed. The uniformity of lifetime in the 10 rods bombarded simultaneously was always better than 25%. The results for all n -type samples, together with Wertheim's data,⁷ are plotted in Fig. 1. His determination of the capture cross section and of the energy level of the recombination centers permits the conversion of the data for lifetimes of various n -type resistivities to equivalent lifetimes at 7 ohm cm. A close agreement is observed as based on the single-level picture. In the case of p -type crystals, the data scatter more and cannot be interpreted that simply.

b. Annealing

Typical annealing results are shown in Figs. 2 to 5 for crystal No. 1 in Table I. Figure 2 represents a plot of lifetime as a function of time for samples annealed at different temperatures. The temperatures investigated covered a range between 200° and 400°C. No annealing was detected for temperatures below 100°C in times up to several days. For the analysis, the frac-

tion, f , of defects not annealed at time, t , is of interest. This fraction is defined as

$$f = N(t)/N_b, \quad (1)$$

where $N(t)$ = density of defects remaining at time t , and N_b = density of defects before annealing. As pointed out before, for low densities, the changes of reciprocal lifetime will be proportional to changes in the density of defects. With this we can write

$$f = \left(\frac{1}{\tau(t)} - \frac{1}{\tau_0} \right) / \left(\frac{1}{\tau_b} - \frac{1}{\tau_0} \right) = \frac{\tau_b [\tau_0 - \tau(t)]}{\tau(t) (\tau_0 - \tau_b)}, \quad (2)$$

where $\tau(t)$ and τ_b have the same meaning as for $N(t)$ and N_b , and τ_0 represents the original lifetime. The data of Fig. 2 are converted into terms of f and shown in Fig. 3.

Fletcher and Brown¹⁰ treated several possible types of annealing processes which lead to first-order, to error-function, or to second-order relations. The data as presented in Fig. 3 cannot be interpreted by any single mechanism. Only a combination of functions will lead to the observed annealing behavior. Each of these functions will involve a typical time constant, η_i . If the

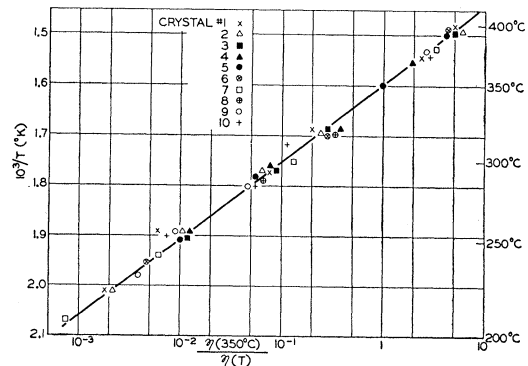


FIG. 5. Time factors leading to superposition as a function of $10^3/T$ for all crystals.

⁹ B. Lax and S. J. Neustadter, J. Appl. Phys. **25**, 1148 (1954).

¹⁰ R. C. Fletcher and W. L. Brown, Phys. Rev. **95**, 585 (1953).

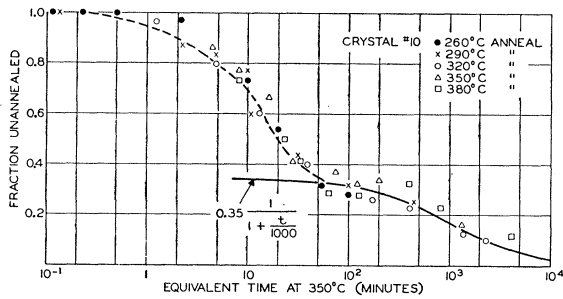


FIG. 6. Data equivalent to those in Fig. 4 for copper-doped crystal (No. 10). Note the increase in the second-order component.

temperature dependence of these different time constants is the same, then it will be possible to multiply the time scale of Fig. 3 by a certain factor and to superpose the annealing points obtained at different temperatures. The points at 350°C have been selected as reference, and superposition leads to Fig. 4. The resulting points all lie on a single curve. Such an analysis has been carried out for all 10 crystals investigated, and the superposition always led to a single resulting curve.

All the time factors thus obtained are shown in Fig. 5. They are plotted as a logarithm of the factor *versus* $10^3/T$. The straight-line relation shows that the time constants involved in the annealing process in all crystals exhibit the same temperature dependence of the form

$$1/\eta_i \propto \exp(-E/kT)$$

with an activation energy, E , of 1.3 ev.

The superposed annealing curves as presented in Fig. 4 for crystal No. 1 should be analyzed in terms of possible annealing processes. The tail of the annealing curves can be attributed only to a second-order process of the general form:

$$f_s = c_s / (1 + t\eta_s).$$

The constant c_s , gives the fraction of defects, which anneal by the second-order process with the time constant, η_s . The constants, c_s and η_s , can be obtained by curve fitting as indicated in Fig. 4. The values for c_s and η_s for all crystals are given in Table I.

The first part of the annealing curve might be associated with any combination of a first-order process, an error-function process, or other type of processes.¹¹ The experimental errors in the lifetime measurements give rise to a fairly large uncertainty in the first part of the annealing cycle. On the basis of the present data

¹¹ J. W. Glen, in *Advances in Physics* (Taylor and Francis, Ltd., London, 1956), Vol. 4, p. 318.

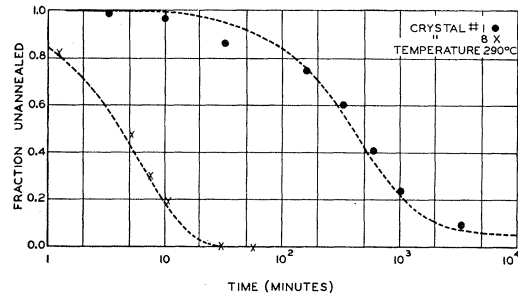


FIG. 7. Comparison of annealing at 290°C between an average pulled crystal (No. 1) and the floating-zone crystal grown in hydrogen (No. 8). Note the fast annealing rate in crystal No. 8.

it appears, therefore, inconclusive to distinguish between the various possibilities, although a single first-order process, together with the above-mentioned second-order component, gives a reasonable fit to the observed curves.

Discussion and Conclusions

The superposition of the annealing curves leads to a single activation energy of 1.3 ev. This indicates that a common mechanism controls the time constants involved throughout the annealing. In most of the discussed models, these time constants are proportional to the inverse of the lattice-jump frequency. The observed activation energy is, therefore, most likely identical with the activation energy for the lattice-jump frequency.¹²

The second-order component associated with the tail of the annealing curves exhibits time constants which have, qualitatively, the expected inverse dependence on the total electron flux. A higher flux leads to shorter values of the time constant.

The copper-doped crystal (Fig. 6) shows an increase in the fraction of defects which anneal by the second-order process. The crystal grown by the floating-zone method in hydrogen (Fig. 7) anneals at a much faster rate than all other crystals, with no indication of a second-order process. The data for these crystals suggest that crystal imperfections can affect the annealing. More experiments along these lines will be necessary to determine the exact nature of the annealing process.

IV. ACKNOWLEDGMENTS

We wish to thank Dr. W. L. Brown, Dr. F. M. Smits, and Dr. G. Wertheim for helpful discussions, Dr. H. Bridgers and Mr. E. Buehler for supplying the silicon crystals used in these experiments.

¹² R. C. Fletcher and W. L. Brown found 1.6 to 1.8 ev for germanium (reference 10).